

Circulation of solids and gas bypassing in an internally circulating fluidized bed with a draft tube

Byung Ho Song¹, Young Tak Kim, Sang Done Kim*

Department of Chemical Engineering and Energy and Environment Research Center, Korea Advanced Institute of Science and Technology, Taejeon 305-701, South Korea

Received 26 September 1996; revised 4 April 1997; accepted 25 April 1997

Abstract

The effects of gas distributor, draft tube height, gas velocity and gap height on the circulation rate of solids and gas bypassing between the draft tube and annulus sections have been determined in a circulating fluidized bed (internal diameter, 0.3 m; height, 2.5 m) with a draft tube (internal diameter, 0.1 m). Gas bypassing strongly depends on the type of gas distributor used for annulus aeration. Gas bypassing from the draft tube to the annulus decreases with increasing draft tube height. The circulation rate of solids is enhanced by gas bypassing from the annulus to the draft tube section regardless of the distributor type. A conical plate distributor with tuyères is found to be the most suitable configuration for the circulation of solids in the circulating fluidized bed with a draft tube. The solids circulation rate obtained has been correlated with the pressure drop across the gap opening and the opening ratio using the orifice equation. © 1997 Elsevier Science S.A.

Keywords: Solids circulation rate; Gas bypassing; Draft tube; Circulating fluidized bed

1. Introduction

Circulating fluidized beds have been widely used in coal combustion and gasification and petroleum refining processes. However, conventional circulating fluidized beds require a very tall main vessel as a solids riser and an accompanying tall cyclone. To reduce the height of conventional circulating fluidized beds and construction costs, several new types of circulating fluidized bed, using a draft tube to divide the bed for internal circulation of solids in a single vessel, have been developed [1–4]. The use of a fluidized bed with a draft tube for internal circulation of solids, with separate aeration of the annulus region, may provide more flexible operation. A schematic diagram of the system is shown in Fig. 1(a). The particles are always transported upwards in the draft tube and move downwards in the annulus section. The gas velocities in the draft tube and annulus sections are different from the given gas velocities with different gas distributors due to gas bypassing between the draft tube and annulus sections. Gas bypassing can be controlled by the inlet geometry of the draft tube [4]. The circulation rate of solids

in the bed can be easily controlled by adjusting the gas velocities to the draft tube and annulus sections independently. In addition, it has been reported that particle entrainment from the reactor can be reduced by the addition of a draft tube to the fluidized bed [5–7]. Thus a consequent increase in the conversion level can be expected compared with conventional fluidized beds. Therefore, a fluidized bed reactor with a draft tube may provide a higher thermal efficiency as a coal gasifier. In such a reactor, gas streams can be fed into the draft tube and annulus zones, so that the draft tube zone can be operated as a slugging/turbulent fluidized bed and the annulus zone as a moving bed at the incipient fluidizing condition. In addition, circulation of solids within the reactor provides heat transfer from the combustion to gasification zones. Therefore the hydrodynamic properties, such as the circulation rate of solids and gas bypassing must be determined to provide the necessary information for the design of a circulating fluidized bed with a draft tube. In this study, the effects of the gas velocity to the draft tube (fluidized bed) and annulus (moving bed), distributor type (bubble cap, ring sparger, conical tuyère), height of the draft tube and gap height on the circulation rate of solids and gas bypassing have been determined. In addition, a relationship is developed between the circulation rate of solids and gas bypassing fractions in the beds.

* Corresponding author.

¹ Present address: Department of Chemical Engineering, Kunsan National University, Kunsan, South Korea.

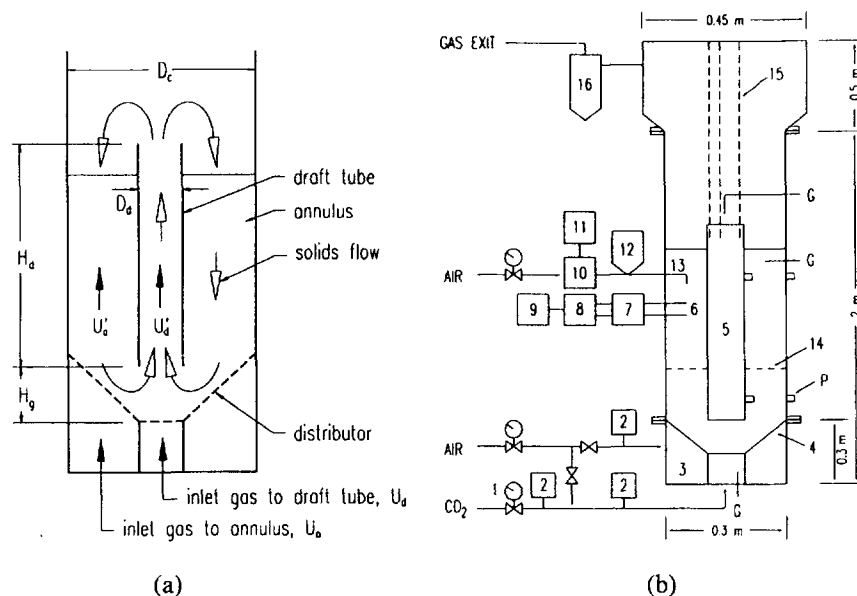


Fig. 1. (a) Schematic diagram of an internally circulating fluidized bed; (b) experimental apparatus: 1, pressure regulator; 2, flow meter; 3, air box; 4, gas distributor; 5, draft tube; 6, thermistor probe; 7, bridge circuit; 8, data acquisition system; 9, personal computer; 10, solenoid valve; 11, timer; 12, hopper; 13, tracer injection tube; 14, three horizontal bars fixing the draft tube; 15, three steel bolts for vertical movement of the draft tube; 16, cyclone; G, gas sampling port; P, to pressure transducer and manometer.

2. Experimental details

2.1. Equipment

Experiments were carried out in a Plexiglas column (internal diameter (i.d.), 0.3 m; height, 2.5 m) with a centrally located draft tube (i.d., 0.1 m; height, 0.3 or 0.6 m) as shown in Fig. 1(b). The freeboard region was expanded (i.d., 0.45 m; height, 0.5 m) to reduce particle entrainment. The bed was loaded with a known weight of sand particles ($d_p = 0.3$ mm, $\rho_s = 2620$ kg m⁻³, $U_{mf} = 0.1$ m s⁻¹, $\epsilon_{mf} = 0.48$) to provide the initial static bed height, according to the draft tube height, and fluidized by compressor air through a pressure regulator, a filter and one of two calibrated gas flow meters. In the bed, one of two different draft tubes was installed. The distance or gap height between the distributor plate and the draft tube inlet was adjusted by varying the height of three steel bars bolted on the top of the draft tube. Two pressure taps were mounted flush to the walls of the column and the draft tube. The pressure taps were connected to differential pressure transducers which measured the pressure drops across the fluidized bed, the moving beds and the gap opening (between the draft tube inlet and the bottom of the annulus). At the bottom of the bed, one of three different gas distributors was mounted on the distributor box to supply air into the draft tube and annulus independently. The bubble cap distributor was used for gas supply to the draft tube. For gas supply to the annulus zone, three different gas distributors were tested (Fig. 2), namely a flat plate bubble cap distributor containing 12 bubble caps (4 holes \times 2.5 mm i.d. in each bubble cap), a conical plate with an inclined angle of 60° relative to the horizontal plane with 18 tuyères (4 holes \times 1.5 mm i.d. in each tuyère) and a double-ring sparger made of 8 mm i.d.

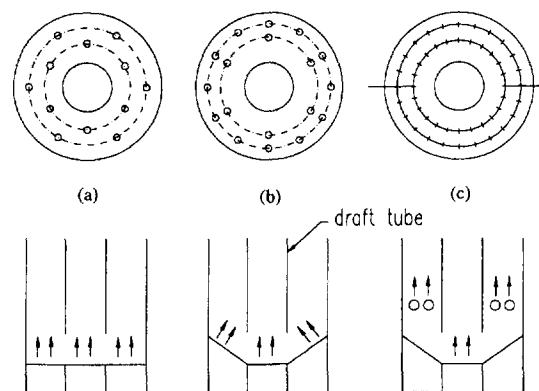


Fig. 2. Top and side views of the three gas distributors: (a) flat plate bubble caps; (b) conical plate tuyères; (c) conical plate ring sparger.

copper tube (22 \times 1.5 mm i.d.), 50 mm above the bottom of the draft tube in the annular section, to reduce gas bypassing from the annulus to the draft tube section; the location of the latter was somewhat higher than that of the other distributors. Therefore we can compare the data obtained from the double-ring sparger qualitatively with those from the other distributors employed.

2.2. Measurement of gas bypassing

Since a fluidized bed with a draft tube has two gas inlets and two gas outlets, the amount of bypassed gas flowing into the annulus and draft tube zones must be determined. A tracer gas (CO₂) was continuously injected into the inlet gas stream to the draft tube, and gas samples were taken at the draft tube inlet and at the outlets of the draft tube and annulus sections. The samples were analyzed using gas chromatography (HP-5840A). Using the four gas concentrations (the CO₂ concen-

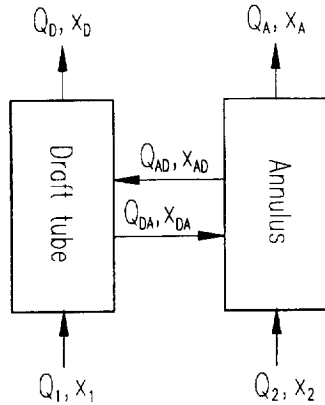


Fig. 3. Mass balance for calculating the gas bypassing fraction.

tration of the inlet gas to the annulus is equal to zero since no tracer was injected into the inlet gas stream to the annulus) and the two inlet gas flow rates, the splitting of the two inlet gases flowing into the other region can be determined; the material balance of the two regions in the system is given in Fig. 3. The bypassing fraction of the inlet gas (f) is defined as the vol.% of the inlet gas bypassed to the other region; the bypassing fraction of the inlet gas of the draft tube to the annulus zone is

$$f_{DA} = 100(Q_{DA}/Q_1) \quad (1)$$

where the subscript DA denotes gas bypassing from the draft tube to the annulus. Assuming that the tracer concentration of the bypassed gas is identical to that of the corresponding inlet gas, the four unknown flow rates (Q_D , Q_A , Q_{DA} , Q_{AD}) can be calculated from the mass balances. The total mass balance for the two regions is

$$\{\rho_g(1-x_1) + \rho_c x_1\}Q_1 + \{\rho_g(1-x_2) + \rho_c x_2\}Q_2 = \{\rho_g(1-x_D) + \rho_c x_D\}Q_D + \{\rho_g(1-x_A) + \rho_c x_A\}Q_A \quad (2)$$

The CO₂ mass balance for the two regions is

$$\rho_c x_1 Q_1 + \rho_c x_2 Q_2 = \rho_c x_D Q_D + \rho_c x_A Q_A \quad (3)$$

where $x_2=0$, since no tracer was injected into the annulus inlet. From Eqs. (2) and (3), Q_D and Q_A can be obtained. The total mass balance for the draft tube region is

$$\begin{aligned} & \{\rho_g(1-x_{AD}) + \rho_c x_{AD}\}Q_{AD} + \{\rho_g(1-x_1) + \rho_c x_1\}Q_1 \\ & = \{\rho_g(1-x_{DA}) + \rho_c x_{DA}\}Q_{DA} + \{\rho_g(1-x_D) + \rho_c x_D\}Q_D \end{aligned} \quad (4)$$

where $x_{AD}=x_2=0$ and $x_{DA}=x_1$. The CO₂ mass balance for the draft tube region is

$$\rho_c x_2 Q_{AD} + \rho_c x_1 Q_1 = \rho_c x_1 Q_{DA} + \rho_c x_D Q_D \quad (5)$$

Therefore Q_{DA} and Q_{AD} can be calculated from Eqs. (4) and (5) respectively.

2.3. Measurement of the circulation rate of solids (W_s)

The circulation rate of solids was determined by measuring the particle downward velocity in the moving bed. Heated bed material was used as a tracer to measure the particle downward velocity in the moving bed using two thermistor probes. The probes were installed in the moving bed, 0.30 and 0.34 m above the distributor. A known volume of heated sand particles (250 °C) was injected pneumatically by impulse into the annulus section through an L-shaped injection tube, 0.2 m below the bed surface. When hot sand particles contacted the probe, a change in resistance of the probe was converted into voltage through a bridge circuit and amplified and stored in a personal computer. By measuring the time lag (τ) between the peak-to-peak distance of two sharp signals, the particle downward velocity can be estimated from the known distance between the two probes (L) divided by the time lag ($V_a = L/\tau$). It was assumed that the measured particle velocity at the center of the annulus represented the average bulk velocity in the annulus [8].

The circulation rate of solids can be calculated from the relation

$$W_s = \rho_s(1 - \varepsilon_a) V_a \quad (6)$$

where ρ_s , ε_a and V_a are the density of solids, bed voidage and bulk velocity of the particles in the moving bed respectively; ε_a was assumed to be the bed voidage at the minimum fluidizing condition (ε_{mf}). The experimental variables and their ranges are summarized in Table 1.

Table 1
Ranges of the experimental variables

	Gas distributor for annulus gas supply		
	Flat bubble cap	Ring sparger	Conical tuyère
Opening area ratio ^a	0.30	0.09	0.28
Draft tube height (mm)	300	300	300, 600
Gap height (mm)	65–200	80	80, 140
Static bed height (mm)	365–465	380	380, 680, 740
Annulus inlet gas velocity, U_a/U_{mf}	0.4–1.6	0.5–1.0	0.5–1.6
Draft tube inlet gas velocity, U_d/U_{mf}	2.6–8.7	8.0–15.6	5.4–20.4

^aRatio of opening area fraction of the distributors to annulus and draft tube.

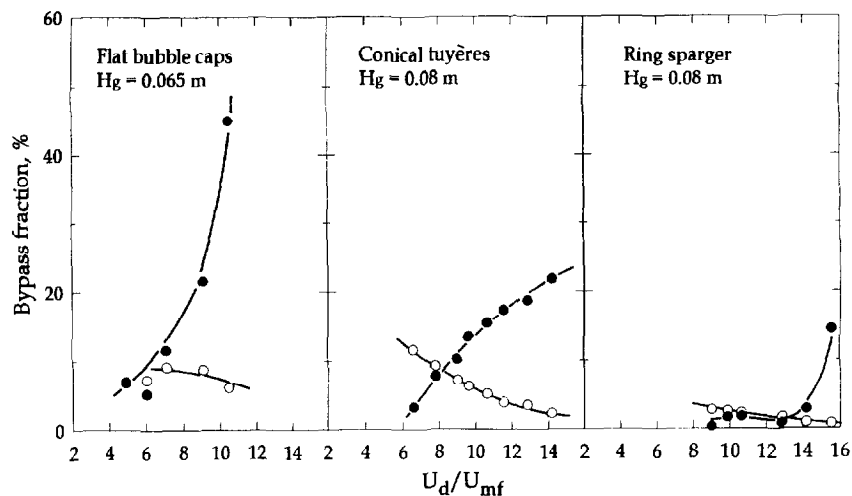


Fig. 4. Effect of U_d on the gas bypassing fraction ($U_a/U_{mf} = 0.7$): ●, f_{AD} ; ○, f_{DA} .

3. Results and discussion

3.1. Gas bypassing

In a circulating fluidized bed with a draft tube for coal gasification, steam is introduced into the annulus (moving bed) and the combustion agent (air) is fed to the draft tube (fluidized bed). However, if a large amount of air bypasses into the gasification zone, coal combustion will dominate in the two reaction zones in a circulating fluidized bed coal gasifier with a draft tube. Therefore, the cross flow of the reactant gases should be minimized between the two reaction zones to obtain the desired product gas quality. Since the inlet gas pressure at the draft tube is lower than that at the bottom of the annulus, the inlet gas flow to the annulus will bypass to the draft tube. Reverse gas bypassing from the draft tube to the annulus is also possible. If this phenomenon occurs, the circulation rate of solids will be reduced below the intrinsic rate due to the countercurrent flow of the solid and gaseous phases.

The effect of the inlet gas velocity to the draft tube (U_d) on the bypassing fractions of the inlet gases to the draft tube and annulus (f_{AD} and f_{DA}) is shown for each gas distributor in Fig. 4. It was found previously [9], with a flat bubble cap distributor, that a variation of the gap height (65–80 mm) has little effect on gas bypassing. Although f_{AD} increases rapidly to 50% with increasing U_d with a flat bubble cap distributor, f_{AD} with a conical tuyère distributor gradually increases up to 15% at $U_d/U_{mf} = 10$. This gas bypassing trend is consistent with that of the pressure drop across the gap opening (ΔP_o) with increasing U_d . With a conical tuyère distributor, ΔP_o exhibits a maximum value at around $U_d/U_{mf} = 10$, whereas ΔP_o increases continuously with U_d with a flat plate bubble cap distributor. Therefore an increase in ΔP_o provides easy gas bypassing from the annulus to the draft tube. The circular ring sparger provides the lowest gas bypassing (less than 5%), since the location of the distributor is 5 cm higher compared with the other distributors employed. However, when U_d/U_{mf} reaches about 14, f_{AD} begins to

increase beyond the 5% level. Gas bypassing from the annulus depends on the opening area ratio in the distributors for the annulus and draft tube sections (Table 1). Thus a small opening area ratio can reduce gas bypassing from the annulus to the draft tube. The gas bypassing fractions (f_{DA}) from the draft tube to the annulus section decrease with increasing U_d within the 15% level for all types of distributor employed. The conical tuyère distributor provides the largest f_{DA} at low U_d , with the largest decreasing rate of f_{DA} with increasing U_d .

To examine the dominant gas bypassing direction as a function of U_d for the three different distributors, the flow ratio was defined as the volumetric gas flow rate in the draft tube over that in the annulus. The flow ratios at the inlet ($FR_{in} = Q_1/Q_2$) and outlet ($FR_{out} = Q_D/Q_A$) of the bed are plotted in Fig. 5, where $FR_{out} > FR_{in}$ indicates the dominant gas bypassing direction from the annulus to the draft tube. As can be seen, gas bypassing from the annulus to the draft tube dominates at the given gas velocities. The rate of change of FR_{out} with respect to FR_{in} is largest with the flat bubble cap distributor. The dominant gas bypassing direction is

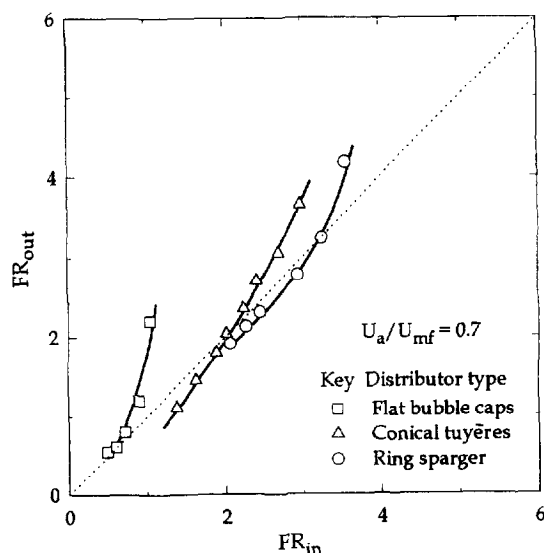


Fig. 5. The outlet to inlet flow ratio for the three different gas distributors.

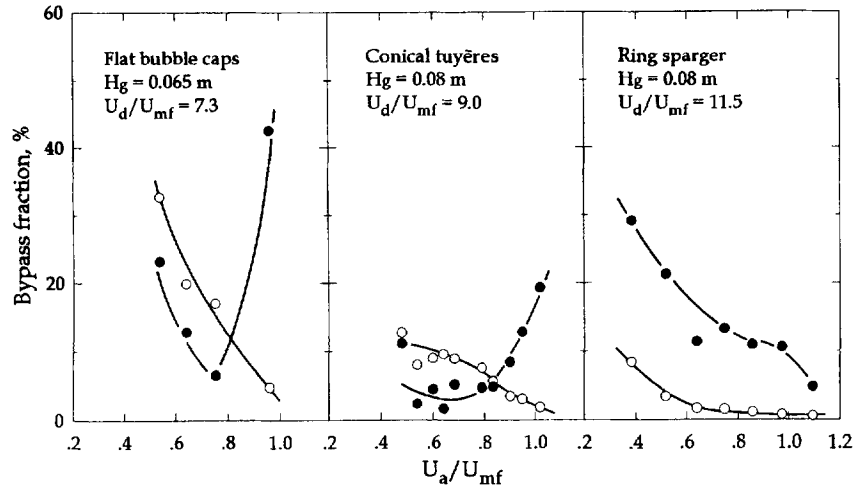


Fig. 6. Effect of U_a on the gas bypassing fraction: ●, f_{AD} ; ○, f_{DA} .

reversed at a certain flow ratio with the ring sparger and conical tuyère distributors. $FR_{out} = FR_{in}$ does not mean that there is no gas bypassing.

The effect of the inlet gas velocity to the annulus (U_a) on the gas bypassing fraction for each gas distributor is shown in Fig. 6. A qualitative comparison of the gas bypassing trends of the three gas distributors can be seen in this figure at different U_d/U_{mf} values. As observed in Fig. 4, f_{AD} with the flat bubble cap distributor is larger than that with the conical tuyère distributor at a given U_d/U_{mf} value. With lower U_d/U_{mf} ($=7.3$) values, f_{AD} with the flat bubble cap distributor is still larger than that with the conical tuyère distributor (Fig. 6). For the ring sparger, smooth circulation of solids occurs and reproducible bypassing data can be obtained at $U_d/U_{mf} > 11$. The f_{AD} values at $U_d/U_{mf} = 11.5$ were chosen for comparison. A minimum value of f_{AD} is obtained at $0.6 < U_a/U_{mf} < 0.8$ with the flat bubble cap and conical tuyère distributors. Visual observations show that solids in the annulus section are in the fixed bed state and do not circulate at $U_a/U_{mf} < 0.6$. Since resistance to gas flow through a packed bed of solids is large, gas fed to the annulus section flows into the draft tube. At $U_a/U_{mf} > 0.6$, the solids start to circulate to form a moving bed in the annulus section. The free void space between the moving particles in the annulus may reduce f_{AD} . At $U_a/U_{mf} > 0.8$, f_{AD} begins to increase with increasing U_a due to increasing solid entrainment from the bottom of the annulus to the draft tube inlet. As U_a is increased further, solids in the annulus section approach the minimum fluidization state and circulation becomes faster through the loop. Since the solids in the annulus section are in the moving bed state the gas supplied can easily percolate through them and f_{AD} decreases. Since the ring sparger for annulus gas supply is located at a higher level than the other distributors, solids below the ring sparger are under the minimum fluidization state. Consequently, circulation of solids does not increase appreciably, and f_{AD} does not increase with increasing U_a/U_{mf} above 0.8. In contrast, f_{DA} decreases monotonically with increasing U_a and U_d with the three different distributors. The largest f_{DA} at low U_a is obtained with the

flat bubble cap distributor, and the ring sparger exhibits the lowest f_{DA} . On the basis of the experimental findings, the conical plate distributor is better than the other two types of distributor for annulus aeration. The flat bubble cap distributor produces the largest gas bypassing fraction of the tested distributors. Although gas bypassing can be reduced with the circular ring sparger, the flexibility with respect to the operating gas velocity is limited.

The effects of the inlet gas velocities (U_d and U_a) on f_{AD} and f_{DA} , with the conical tuyère distributor, using two different draft tube heights (H_d) are shown in Figs. 7 and 8. In Fig. 7(a), f_{AD} increases with increasing U_d , whereas in Fig. 7(b), f_{DA} decreases with increasing U_d , at the given U_a/U_{mf} . A small variation in U_a produces a large increase in f_{AD} (about 20% at $U_d/U_{mf} = 12$). As can be seen in Fig. 8(a), f_{AD} exhibits a minimum value at $U_a/U_{mf} = 0.8$ and f_{DA} decreases with increasing U_a and U_d .

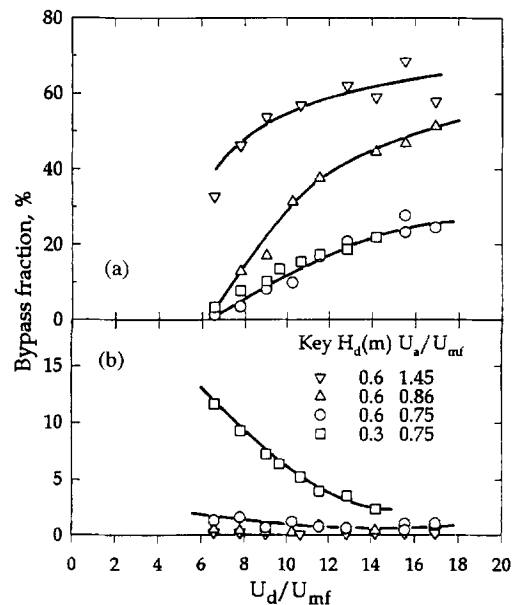


Fig. 7. Effect of U_d on the gas bypassing fraction with the conical tuyère distributor: (a) f_{AD} ; (b) f_{DA} .

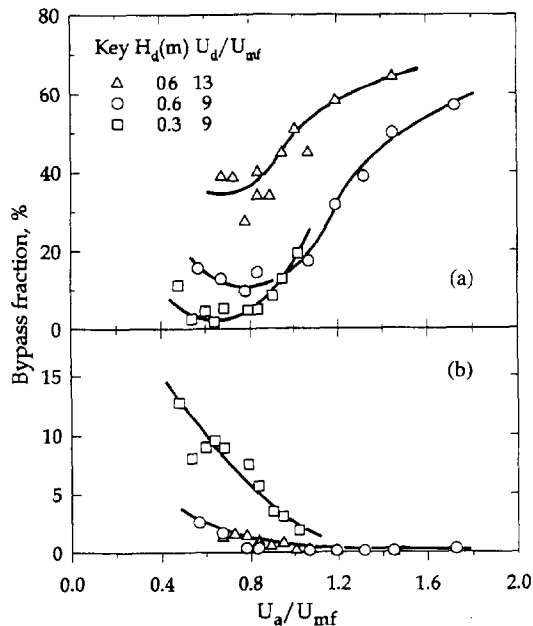


Fig. 8. Effect of U_a on the gas bypassing fraction with the conical tuyère distributor: (a) f_{AD} ; (b) f_{DA} .

The effect of the height of the draft tube (H_d) on f_{AD} is small, but on f_{DA} is significant. With a variation of H_d from 0.3 to 0.6 m, the pressure drop through the annular section increases due to a corresponding increase in the solids inventory in the annular section. An increase in the pressure drop across the gap opening (ΔP_o) interferes with the gas flow from the draft tube to the annulus section and the higher H_d provides a lower f_{DA} (Fig. 8(b)). Therefore f_{AD} can easily be controlled via the operating gas velocities (U_d and U_a) and the draft tube height.

3.2. Circulation rate of solids (W_s)

The effect of U_d on W_s for each gas distributor is shown in Fig. 9. W_s increases with U_d due to the increase in the driving

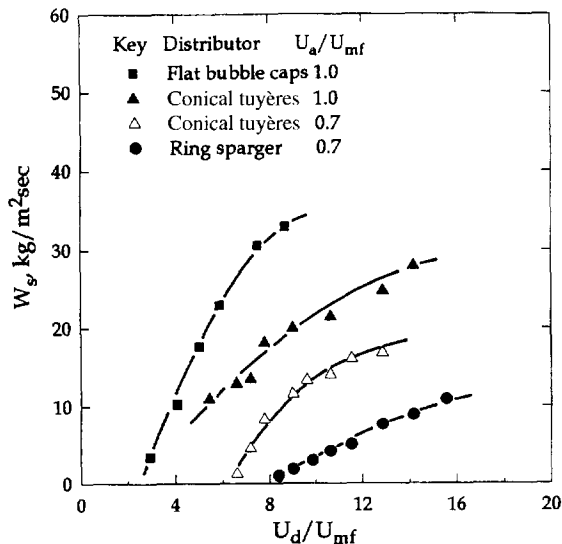


Fig. 9. Effect of U_d on W_s with the three different gas distributors.

force for the circulation of solids between the two beds with an increase in bed voidage in the draft tube. However, at higher U_d , the rate of increase in W_s decreases due to the increase in the backmixing of solids at the draft tube inlet. In addition, solid cluster formation in the dense phase may decrease when the jet diameter is larger than the draft tube diameter at higher U_d [10]. The gas bypassing from the annulus to the draft tube will increase the diameter of the gas jet from the distributor to the draft tube. Therefore W_s should increase with increasing gas bypassing fraction from the annulus to the draft tube even at low U_d . From Figs. 4 and 9, it can be readily seen that the differences in W_s with each gas distributor are similar to the differences in f_{AD} . The magnitudes of W_s and f_{AD} can be ranked as follows: flat bubble cap > conical tuyères > ring sparger (location of the ring sparger is somewhat higher than that of the other distributors).

The effect of U_a on W_s is shown in Fig. 10; W_s increases with increasing U_a regardless of the distributor type. As can be seen, the circulation of solids begins to occur at an aeration velocity of around $U_a/U_{mf} = 0.5$, and W_s at a given U_a is more pronounced with the flat bubble cap distributor compared with the other distributors. This can be related to the gas bypassing phenomena in Fig. 8. At higher U_a , f_{AD} enhances W_s , whereas f_{DA} interferes with the downflow of solids in the annulus. The rate of increase in W_s begins to slow down at around $U_a/U_{mf} = 1.2$, since the difference in density between the two beds is reduced with bubble formation in the annulus section. A similar change in f_{AD} is observed at higher U_a/U_{mf} .

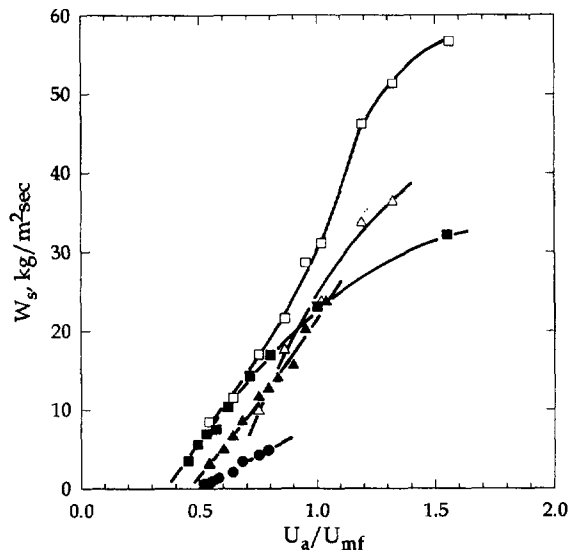


Fig. 10. Effect of U_a on W_s with the three different gas distributors:

Distributor	H_g (m)	H_d (m)	U_d/U_{mf}
□ Conical tuyères	0.14	0.6	9.0
△ Conical tuyères	0.08	0.6	9.0
▲ Conical tuyères	0.08	0.3	9.0
■ Flat bubble caps	0.065	0.3	6.0
● Ring sparger	0.08	0.3	9.9

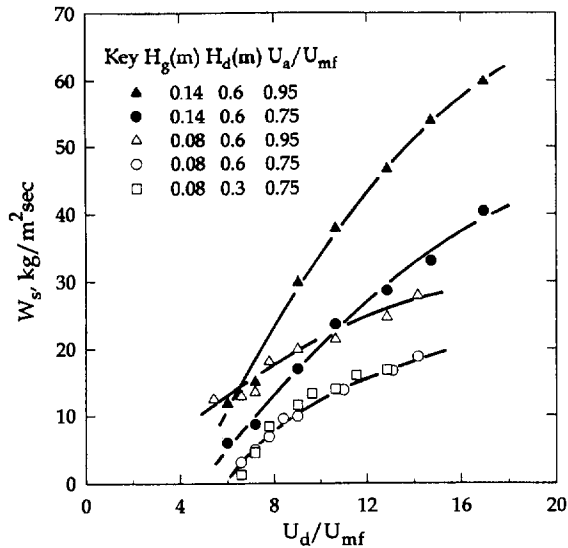


Fig. 11. Effect of H_d and H_g on W_s with the conical tuyère distributor.

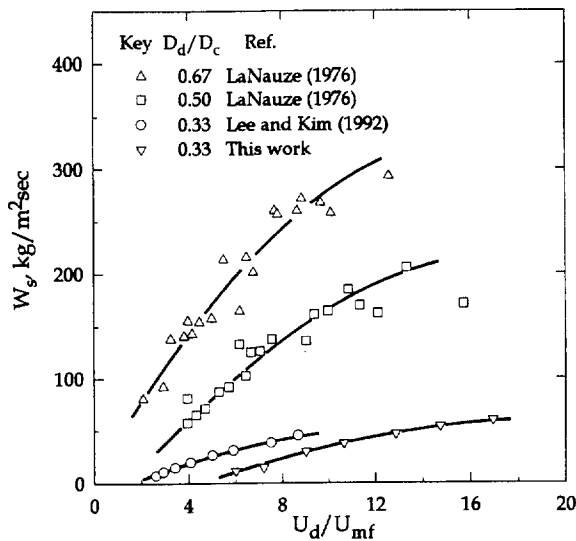


Fig. 12. Effect of D_d/D_c on W_s .

The effects of the draft tube height (H_d) and gap height (H_g) on W_s at the given gas velocities are shown in Fig. 11 with the conical tuyère distributor. As can be seen, the effect of H_d (0.3–0.6 m) on W_s is small. However, W_s increases significantly with increasing H_g . With larger H_g , the resistance to the flow of solids from the annulus to the draft tube will decrease, and a steady increase in W_s can be expected. However, the increase in W_s with H_g may be limited by gas bypassing from the draft tube to the annulus. It has been reported that a start-up problem may occur when H_g is too large [11].

The effect of D_d/D_c on W_s is shown in Fig. 12 (data from this and previous studies [3,9]). The diameter ratio of the draft tube (D_d) to the main column (D_c) may indicate the capacity of the reactor. As expected, a higher W_s can be obtained by using a larger D_d/D_c ratio.

3.3. Prediction of the flow rate of solids

The experimental data clearly indicate that the pressure drop across the gap opening determines the flow rate of solids for a given circulating fluidized bed. The flow rates of particles in the annulus and in the gap opening are related by the following mass balance

$$W_s S_a = W_o S_o = \rho_o V_o S_o \tag{7}$$

The bulk velocity of particles at the opening can be expressed by Bernoulli's equation, as suggested by Judd and Dixon [12]:

$$V_o = C_s \sqrt{\frac{2\Delta P_o}{\rho_o \left[1 - \left(\frac{S_o}{S_a} \right)^2 \right]}} \tag{8}$$

where C_s is the particle discharge coefficient. The bed density at the opening can be assumed to be equal to that in the annulus section, i.e. $\rho_o = \rho_a$.

For non-circular openings and downflowing beds, the opening ratio is defined as

$$r = \frac{S_o}{S_a} = \left(\frac{\text{hydraulic diameter of opening}}{\text{hydraulic diameter of downflowing bed}} \right)^2 \tag{9}$$

Substituting Eqs. (8) and (9) into Eq. (7), the following equation can be obtained:

$$W_s = C_s r \sqrt{\frac{2\rho_a \Delta P_o}{1 - r^2}} \tag{10}$$

The experimental results show that the variation in the bed density in the annulus section as a function of the operating gas velocity is small, with a standard deviation of 12%, whereas ρ_a is mainly affected by the height of the draft tube. Therefore, for a given draft tube, the average value of ρ_a is used in Eq. (10).

The experimental data of W_s in Fig. 13 were analyzed using Eq. (10), which produces different values of C_s according to

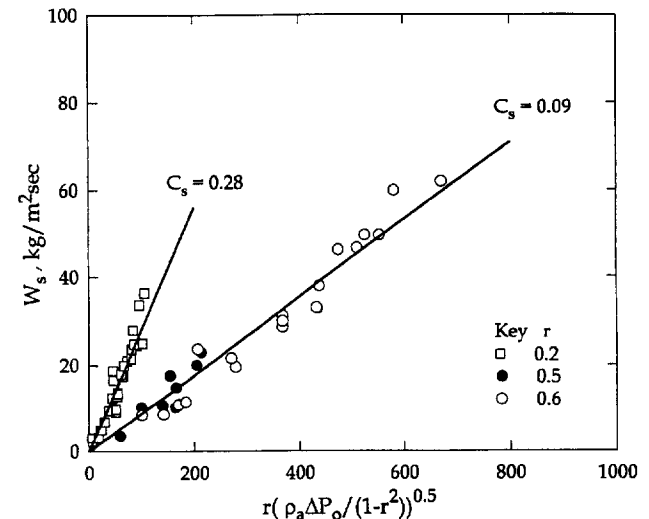


Fig. 13. Correlation for W_s based on the orifice-type equation (Eq. (10)): $1.0 \leq U_a/U_{mf} \leq 1.56$, $3 \leq U_d/U_{mf} \leq 20$.

the opening ratio: 0.28 for $r=0.2$ and 0.09 for $0.5 \leq r \leq 0.6$. It has been shown previously [13] that the effect of the opening ratio on the circulation rate of solids is not clear when the opening ratio is larger than 0.7. Coefficients smaller than 0.1 have frequently been observed in internal circulation systems [13,14]. The circulation rate of solids can be predicted as a function of the pressure drop across the gap opening using Eq. (10). The calculated values and C_s obtained are in close agreement with the experimental data of the present analysis.

4. Conclusions

Gas bypassing from the annulus to the draft tube increases and reverse gas bypassing from the draft tube to the annulus decreases with increasing U_d at a constant U_a , regardless of the gas distributor type. Gas bypassing from the draft tube can be reduced significantly by using higher draft tube heights. It has been found that f_{AD} exhibits a minimum value at $0.6 < U_a/U_{mf} < 0.8$. The difference in W_s , with the three different gas distributors, follows exactly the trends in f_{AD} . On the basis of the gas bypassing and circulation rate of solids with the present operating variables, the conical tuyère distributor is found to be the most suitable for a circulating fluidized bed with a draft tube. The solids circulation rate data are well represented by the orifice equation and can be correlated with the pressure drop across the gap opening and the opening ratio.

Acknowledgements

We acknowledge a grant-in-aid for research from the Ministry of Trade, Industry and Energy, South Korea.

Appendix A. Nomenclature

C_s	particle discharge coefficient of the opening, –
D_d	diameter of draft tube, m
D_c	diameter of main column, m
d_p	mean diameter of particle, m
f	gas bypassing fraction, vol.% of inlet gas bypasses to the other region, –
f_{AD}	gas bypassing fraction from the annulus to the draft tube, %
f_{DA}	gas bypassing fraction from the draft tube to the annulus, %
FR_{in}	flow ratio at the inlet of the bed, $= Q_1/Q_2$
FR_{out}	flow ratio at the outlet of the bed, $= Q_D/Q_A$
H	static bed height, m
H_d	height of draft tube, m
H_g	gap height, m

ΔP_o	pressure drop across the gap opening, Pa
Q_1	gas flow rate at the draft tube inlet, $m^3 s^{-1}$
Q_2	gas flow rate at the annulus inlet, $m^3 s^{-1}$
Q_A	gas flow rate at the annulus outlet, $m^3 s^{-1}$
Q_D	gas flow rate at the draft tube outlet, $m^3 s^{-1}$
Q_{AD}	flow rate of bypassed gas from the annulus to the draft tube, $m^3 s^{-1}$
Q_{DA}	flow rate of bypassed gas from the draft tube to the annulus, $m^3 s^{-1}$
r	opening ratio defined in Eq. (9), –
S_a	cross-sectional area of the annulus bed, m^2
S_o	area of the opening, m^2
U_a	superficial inlet gas velocity to the annulus, $m s^{-1}$
U_d	superficial inlet gas velocity to the draft tube, $m s^{-1}$
U_{mf}	minimum fluidization gas velocity, $m s^{-1}$
V_a	bulk velocity of particles in the annulus bed, $m s^{-1}$
V_o	bulk velocity at the opening, $m s^{-1}$
x	tracer (CO_2) concentration in the gas stream
W_o	circulation rate of solids per unit area of the opening, $kg m^{-2} s^{-1}$
W_s	circulation rate of solids per unit area of the annulus bed, $kg m^{-2} s^{-1}$
ϵ_a	voidage in a downflowing annulus bed, –
ϵ_{mf}	voidage at the minimum fluidization condition, –
ρ_a	bulk density of a downflowing annulus bed, $kg m^{-3}$
ρ_c	density of carbon dioxide, $kg m^{-3}$
ρ_g	density of air, $kg m^{-3}$
ρ_o	bed density at the opening, $kg m^{-3}$
ρ_s	density of solid particle, $kg m^{-3}$

References

- [1] M.St.J. Arnold, J.J. Gale, M.K. Laughlin, *Can. J. Chem. Eng.* 70 (1992) 991.
- [2] J.C. Berggren, I. Bjerle, H. Eklund, H. Karlsson, O. Svensson, *Chem. Eng. Sci.* 35 (1980) 446.
- [3] R.D. LaNauze, *Powder Technol.* 15 (1976) 117.
- [4] W.C. Yang, D.L. Keairns, *Can. J. Chem. Eng.* 61 (1983) 349.
- [5] O. Kinoshita, T. Kojima, T. Furusawa, *J. Chem. Eng. Jpn.* 20 (1987) 641.
- [6] R.K. Riley, M.R. Judd, *Chem. Eng. Commun.* 62 (1987) 151.
- [7] Y.T. Kim, B.H. Song, S.D. Kim, *Chem. Eng. J.* 66 (1997) 105.
- [8] Y.T. Choi, S.D. Kim, *J. Chem. Eng. Jpn.* 24 (1991) 195.
- [9] W.J. Lee, S.D. Kim, in: O.E. Potter, D.J. Nicklin (Eds.), *Fluidization VII*, Engineering Foundation, New York, 1992, p. 479.
- [10] J.R. Muir, F. Berruti, L.A. Behie, *Chem. Eng. Commun.* 88 (1990) 153.
- [11] W.C. Yang, P.J. Margaritis, D.L. Keairns, *AIChE Symp. Ser.* 74 (176) (1978) 87.
- [12] M.R. Judd, P.D. Dixon, *AIChE Symp. Ser.* 74 (176) (1978) 38.
- [13] M. Kuramoto, D. Kunii, T. Furusawa, *Powder Technol.* 47 (1986) 141.
- [14] W.C. Yang, D.L. Keairns, *AIChE Symp. Ser.* 70 (141) (1974) 27.